



DEVELOPMENT OF A 10 KW MICROWAVE APPLICATOR FOR THERMAL CRACKING OF LIGNITE BRIQUETTES

Benjamin Lepers^{a,*}, Thomas Seitz^a, Guido Link^a, John Jelonnek^{a,b}, Mark Zink^c

^aKarlsruhe Institute of Technology, Institute for Pulsed Power and Microwave Technology (IHM), Eggenstein Leopoldshafen, 76344, Germany

^bKarlsruhe Institute of Technology, Institute for Highfrequency Techniques and Electronic (IHE), Karlsruhe, 71131, Germany

^cTU Bergakademie Freiberg, Institute of Energy Process Engineering and Chemical Engineering (IEC), Fuchsmuehlenweg 9, 09599 Freiberg, Germany

ABSTRACT

A compact 10 kW microwave applicator operating at 2.45 GHz for fast volumetric heating and thermal cracking of lignite briquettes has been successfully designed and tested. In this paper, the applicator design and construction are presented together with a sequentially coupled electromagnetic, thermal-fluid and mechanical Comsol model. In a first step, this model allows us to calculate the power density inside the lignite material and the temperature distribution in the applicator for different water flow rates. In a second step, the total stress due to the thermal dilatation, the internal pressure inside the ceramic and the contact pressure from the seals at both ends of the ceramic can be computed. In addition, preliminary experimental results are given and showed a significant mechanical strength weakening of the briquettes with microwave heating.

Keywords: Microwave applicator, microwave heating, thermo elastic model, silicon nitride, lignite, thermal cracking

1. INTRODUCTION

In the framework of a collaborative project between IHM from KIT and IEC from TU Bergakademie Freiberg for microwave heating of lignite briquettes, a 10 kW compact applicator operating at 2.45 GHz has been successfully designed and tested. This applicator delivers volumetric heating to the briquettes which are moving inside a microwave transparent ceramic silicon nitride tube with high mechanical strength. Upstream to this applicator, briquettes are produced from the lignite coal powder with a briquetting press machine Rosin *et al.* (2014). Downstream of this applicator, after being heated by the microwave field, the briquettes are moving toward the gasifier for syngas (mixture of hydrogen and carbon monoxide) production for example. This system allows the transfer of lignite material from the production machine to the gasifier with pressure up to 65 bars. Innovative feeding systems for pressurized gasification reactors are currently being developed by TU Freiberg Bergakademie. Important requirements for such systems are a simple design and high reliability. The briquetting press is a continuously operating machine with mass flow up to 25 t/h. The sealing between the briquetting machine and the gasifier is made by the briquettes plug in the feed channel. It makes the briquetting press a self sealing system Rosin *et al.* (2014).

With fast microwave volumetric heating (the moving briquettes crosses the ceramic tube in 9 s and passes in front the rectangular aperture in 2 s, at the production rate 75 briquettes per minute), thermal cracking was observed together with an increase of the briquette friability. Volumetric heating induces thermal cracking and can be used as a thermal pre-treatment to reduce the energy requirement for grinding or can be used directly as a comminution tool (i.e destruction, breakage) for the lignite

material Batar (2004). High power microwave heating of coal with exposure time of few seconds increases significantly the grindability Binner *et al.* (2014), and consequently is beneficial for the overall efficiency of the gasifier. Microwave heating of lignite is much faster than conventional heating of coal Pickles *et al.* (2014) (with the value $\epsilon_r = 5.48 - 0.73j$ for fresh lignite, the skin depth is about 6 cm). This work presents the design of a microwave applicator used for continuous volumetric heating of lignite briquettes together with a Comsol multiphysics model used to calculate the power density, temperature, displacement and stress field in the applicator parts. In addition, some first experimental results are given.

2. THE APPLICATOR DESIGN

The applicator is made of a silicon nitride (Frialit GP79, Friatec) cylinder inserted in an water cooled aluminum block (Alumec 100, Alcoa) of dimension $32 \times 26 \times 22$ cm as shown in Fig. 1. A rectangular wave guide crosses the aluminum bloc to deliver microwave energy to the lignite material moving inside the ceramic cylinder. Microwave radiation at 2.45 GHz is created in the magnetron and travels through the manual tuner and the wave guide. The applicator input power is up to 10 kW corresponding to 8 – 9 kW of absorbed power by the lignite briquettes (depending of the lignite loss factor, ie water content). A three pin manual tuner element is installed after the magnetron and a variable short circuit wave guide element is installed at the end of the applicator wave guide as shown in Fig. 2. These two elements allow a good transmission of the microwave energy from the applicator to the lignite material load. The measured S_{11} magnitude at 2.45 GHz was below -15 dB. In operation,

* Corresponding author. Email: benjamin.lepers@kit.edu

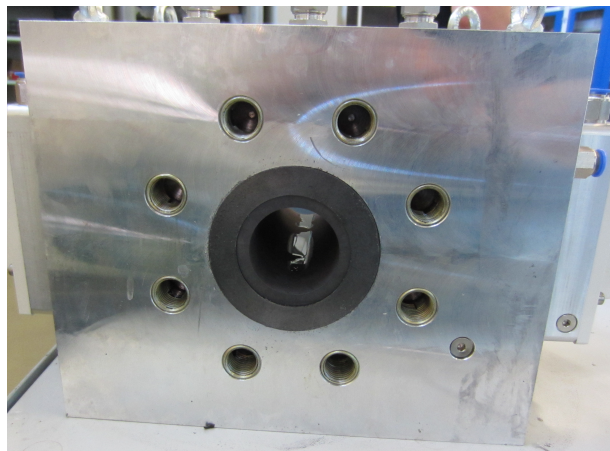


Fig. 1 Aluminum block Alumecc 100 with the ceramic silicon nitride and the graphite seal, the M22 thread insert are visible

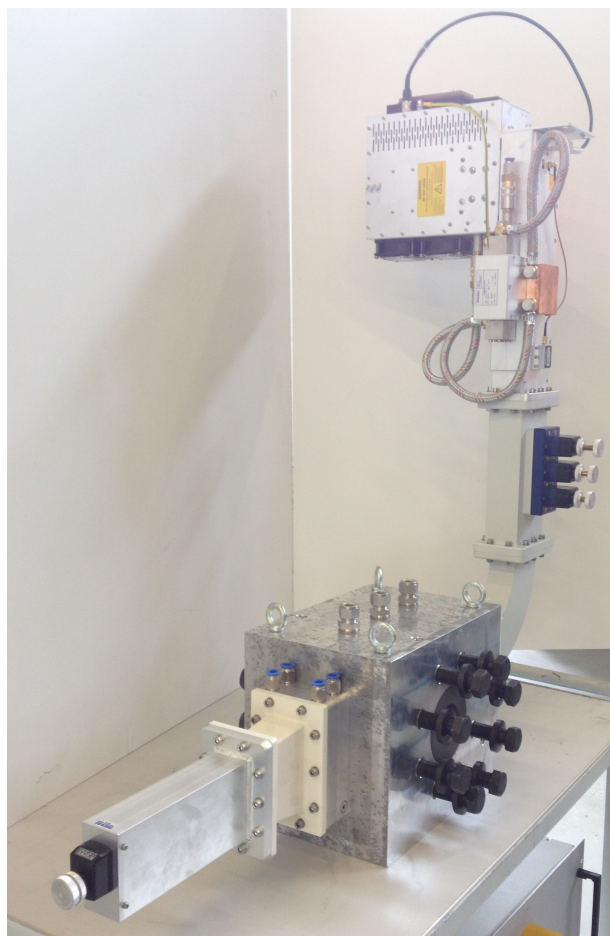


Fig. 2 Applicator with magnetron, manual tuner, aluminum bloc, silicon nitride ceramic, sliding short, wave guide transition (in white) and microwave windows

the measured reflected power was about 2 – 3 % of the input power. To provide significant heating to the lignite briquettes, the following engineering choices were made for this applicator:

- A high mechanical strength and low dielectric loss ceramic was used for the high pressure microwave transparent tube. Silicon nitride (GP79 Friatec) offers these two characteristics with a tensile strength above 400 GPa and a low relative dielectric loss factor around 0.02.
- For an effective sealing, the displacement due to thermal dilatation mismatch between the aluminum frame holder and the ceramic tube has to be minimized. A good solution was found with the aluminum alloy (Alumecc 100, high strength aluminum alloy) together with inner cooling water channels. The high electrical conductivity of aluminum allows the reduction of electrical wall losses, and its high thermal conductivity renders the water cooling system much more efficient than a block made of stainless steel for example. With a water flow rate of 6 l/min the maximum temperature of the aluminum bloc in operation is kept below 45 °C and so the thermal expansion can be limited.
- A compact design which fits near the briquetting press machine installation where limited space is available.

3. CONSTRUCTION

The silicon nitride tube was made by the company Friatec (Silicon nitride GP 79 Hot pressed sintered). The length is 220 mm with inner and outer diameter of 54 and 105 mm respectively. It allows the passage of lignite briquettes of 50 mm in diameter. The aluminum block is made of aluminium alloy Alumecc 100 from the company Alcoa. The machining steps are detailed below:

- the raw aluminum block was cut to the specific dimensions 320 × 260 × 220 mm
- the hole of diameter 105 mm through the depth of the aluminum block (220 mm length) was machined with wire electric discharge machining (EDM, electric discharge that remove the material).
- the rectangular channel of cross section 109 × 54 mm (WR 430 wave guide) was machined with EDM through the 32 cm length of the aluminum block, it intersects the hole of diameter 105 mm made for the ceramic.
- 8 holes of diameter 25 mm were drilled on the two opposite faces of the aluminum block for the thread insert as shown in Fig. 1.
- 3 safety holes of diameter 12 mm with a Swagelock connection type were drilled. In case of over pressure in the space between the outer ceramic tube and aluminum block, the gas will escape through these 3 holes (visible on Fig. 2).
- a cooling circuit inside the aluminium block in the vicinity of the ceramic tube was made by drilling holes of 6 mm in diameter. In total there are 7 straight cooling channel connected. Upstream and downstream, near the ceramic aperture, there are 2 × 3 channels encircling the ceramic tube. One channel is making the connection between the upstream and downstream part of the cooling circuit.

Once all parts were available, the applicator was built by assembling two set of parts. The first set is made of the magnetron head and the manual tuner which is used to minimize the reflected power. The second set is made of a 90 ° right angle wave guide (because of space limitation on the installation site), the transition wave guide and the microwave windows which are screwed on each side of the aluminum block at the rectangular channel location. In addition, a sliding short is screwed to the transition

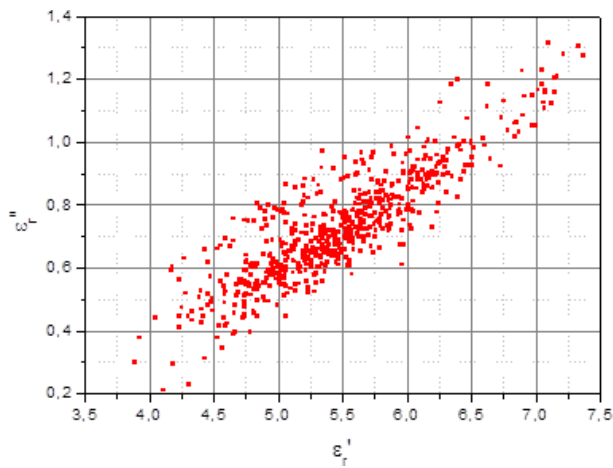


Fig. 3 Real and imaginary part of the relative complex permittivity of Braun coal for 100 briquettes with grain size smaller than 10 mm and water content of about 18 % in mass. The average value used for the electromagnetic simulation is $\epsilon_{rc} = 5.48 - 0.73j$

Properties	Lignite	Silicon nitride	Alumec 100
Relative complex dielectric constant ϵ_{rc} [-]	5.48 – 0.73j	8 – 0.02j	–
Density ρ [kg/m ³]	1200	3200	2850
Thermal conductivity k [W/(mK)]	0.3	21	160
Specific heat C_p [J/(kg.K)]	1200	700	880
Thermal expansion coeff α [10 ⁻⁶ /K]	–	2.3	23
Elastic young modulus E [GPa]	–	320	70
poisson coefficient ν [-]	–	0.28	0.33

Table 1 Dielectric, thermal and mechanical properties for the lignite coal, silicon nitride and Aluminum material used in the sequentially coupled model

wave guide. The sliding short is a tuning element and can minimize the reflected power by adjusting the location of the short circuit. This sliding short works in combination with the manual tuner. The transition wave guide parts have a conical geometry and make the transition from a WR 340 (86 × 43 mm) to a WR 430 (109 × 54 mm) rectangular standard wave guide.

4. MATERIAL PROPERTIES

The electromagnetic, thermal and mechanical properties of the lignite (Romonta), Silicon nitride GP 79 (Friatec) and Aluminum Alumec 100 (Alcoa) were assumed constant and are given in the Tab. 1 (Properties expressed as a function of the temperature will rend the model non linear, and do not bring much more information in the design phase of the applicator). Lignite is a semi mineral organic material consisting of Carbon (73 %), oxygen (20 %), hydrogen (5 %) and nitrogen (1.2 %). Since the briquettes are made from brown coal powder, the material is homogeneous and isotropic at a macroscopic scale and so the real and imaginary part of the complex permittivity are scalar number. For the simulation, the relative permittivity used is $\epsilon_r = 5.48 - 0.73j$ and is obtained from the averaging of the dielectric measurements of fresh lignite briquettes (with water content) performed in our laboratory (see Fig. 3). For the ceramic tube, a silicon nitride (GP 79, Friatech) was chosen because of a very high mechanical strength and low dielectric losses. For the aluminum block, the high strength aluminum Alumec 100 alloy was the best choice, because of a good electrical and thermal conductivity together with a high mechanical strength. In addition, Aluminum alloys are materials easy to be machined.

5. MICROWAVE AND THERMAL MODEL

A standard waveguide WR 430 intersecting with the silicon nitride tube was modelled with Comsol 4.3 to compute the S_{11} magnitude ($|S_{11}|_{dB} = 10 \log(\frac{P_r}{P_i})$, with P_r and P_i the reflected and incident power), the electric field \mathbf{E} and the power density q distribution by solving the wave equation

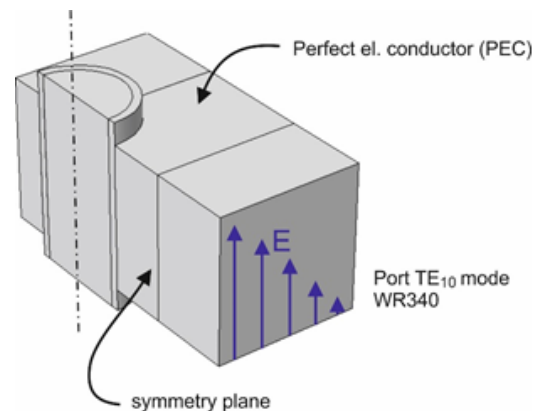


Fig. 4 Electromagnetic model with boundary conditions, from the geometry and field symmetry, only one half is modelled

in the frequency domain at 2.45 GHz:

$$\frac{1}{\mu_r} \nabla \times (\nabla \times \mathbf{E}) - k_0^2 \epsilon_{rc} \mathbf{E} = 0 \quad (1)$$

$$k_0^2 = \omega^2 \mu_0 \epsilon_0$$

$$\epsilon_{rc} = \epsilon_r' - j \epsilon_r''$$

$$q = \frac{1}{2} \omega \epsilon_0 \epsilon_r'' \mathbf{E}^2$$

with k_0 the wave number in free space, ϵ_{rc} the relative complex dielectric permittivity, $\omega = 2\pi f$ the pulsation and q the power density calculated from the electric field. Lignite is a non magnetic material so the relative magnetic permeability is $\mu_r = 1$. $\mu_0 = 4\pi \times 10^{-7}$ H/m and $\epsilon_0 = 8.854 \times 10^{-12}$ F/m are respectively the permeability and permittivity of free space. Using the symmetry of the applicator and of the fundamental mode TE_{10} , only half of the applicator geometry was modelled. On the symmetry plane, a perfect magnetic wall is used (tangential components of the magnetic field do not exist in this plane, $\mathbf{n} \times \mathbf{H} = 0$). On both ends of the ceramic a perfect electric boundary condition was used ($\mathbf{n} \times \mathbf{E} = 0$), because of the electrical conductive graphite seal. The aluminum walls were also assumed to be perfect electric conduc-

tors. A scattering boundary condition was used on both surfaces where the lignite enters and exits the ceramic tube. The boundary conditions for the electromagnetic model are shown in Fig. 4. With some quarter wave length matching elements inserted inside the wave guide, it was possible to achieve a good transmission of the energy from the wave guide to the lignite briquettes. Later, during the applicator development process, the matching elements inserted inside the wave guide were removed and an external manual three pin tuner was used instead. In a second step, the power density q obtained from the electromagnetic model was used to compute with the heat equation the temperature distribution inside the lignite material and the ceramic tube. The effect of the moving briquettes at constant velocity \mathbf{v} inside the ceramic tube was included with the option "translational motion" in the Comsol thermal model. This effect is modelled by the transport term $\rho C_p \mathbf{v} \cdot \nabla T$ shown in Eq. 2. The temperature field in the lignite, and ceramic domain is obtained by solving the heat equation:

$$\rho C_p \frac{\partial T}{\partial t} + \rho C_p \mathbf{v} \cdot \nabla T = \nabla \cdot (k \nabla T) + q \quad (2)$$

with ρ , C_p and k the density, specific heat and thermal conductivity of the material.

6. THERMO-MECHANICAL MODEL

A thermo mechanical model was developed in order to compute the von Mises stress in the two critical parts of the applicator: the ceramic tube and the aluminum bloc. The ceramic is submitted to three source of mechanical stress.

- The non uniform temperature distribution inside the ceramic wall leads to thermal stress.
- A graphite joint is used on both end face of the ceramic tube, with an axial stress of 50 MPa for a good sealing,
- The internal pressure during the process can reach 65 bars.

With a 3-D mechanical model, the total stress was computed with the thermal stress (due to the temperature gradient) and with two pressure boundary conditions on the inner wall of the ceramic and on both flat surfaces. The mechanical model is based on force equilibrium of solids (or Newton law extended to solids):

$$\rho \ddot{\mathbf{u}}(\mathbf{x}, t) - \nabla \cdot \boldsymbol{\sigma}(\mathbf{x}, t) - \boldsymbol{\kappa}(\mathbf{x}, t) = 0 \quad (3)$$

with ρ the density of the solid, \mathbf{u} the displacement vector, $\boldsymbol{\sigma}$ is the material stress tensor for small deformation. $\boldsymbol{\kappa}$ is the external volume forces such as gravity. In our case, the gravity can be neglected in comparison to the internal thermal stress. In addition, the inertial term $\rho \ddot{\mathbf{u}}$ is neglected in comparison to the thermal stress because the time of the duration of the "heat pulse" (microwave heating about 1–3 s) is much larger than the characteristic time of propagation of stress waves inside the solid (speed of sound in the material over a characteristic length of the solid). The equation (3) without the inertial term is also called the quasi static approximation equilibrium of solids. The constitutive law between the stress and the strain used to model the behaviour of the ceramic and the metal parts is a linear elastic model or generalised 3D Hooke's law:

$$\boldsymbol{\sigma} = \frac{E}{1+\nu} \boldsymbol{\epsilon} + \frac{E\nu}{(1+\nu)(1-2\nu)} \text{tr}(\boldsymbol{\epsilon}) \mathbf{I} - \alpha \frac{E}{1-2\nu} \Delta T \mathbf{I} \quad (4)$$

Three parameters are used to define the relationship between the strain $\boldsymbol{\epsilon}$ and the stress $\boldsymbol{\sigma}$ in the case of thermal expansion with a temperature difference ΔT . The Young modulus E , which represents the stiffness of the

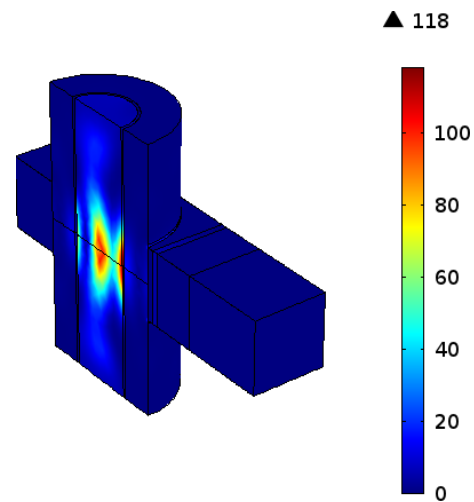


Fig. 5 Power density [MW/m^3] for 10 kW input power

material, the poisson ratio ν which is the ratio between longitudinal and lateral displacement, and the linear thermal expansion coefficient α . The Von Mises stress $\sigma_m = \frac{1}{\sqrt{2}} \sqrt{(\sigma_1 - \sigma_2)^2 + (\sigma_2 - \sigma_3)^2 + (\sigma_3 - \sigma_1)^2}$, is a convenient scalar quantity used to evaluate the stress state inside the solid and to compare with the maximal material strength. σ_i are the main stress components of the stress tensor.

7. THERMAL AND FLUID MODEL

The velocity field inside the water channels was computed with the laminar flow physics of Comsol (Navier stokes equation for an incompressible fluid in laminar regime) in steady state. Then, the thermal model was solved in the solid and in the fluid domain. To take into account the heat transfer from the solid domain to the fluid domain, the advection term $\mathbf{v} \rho C_p \cdot \nabla T$ is used with \mathbf{v} the velocity field obtained with the steady laminar incompressible fluid simulation.

Comment: The author had also the opportunity to test the pipe flow module in Comsol. The calculated temperature field in the solid domain (aluminum block) was similar for both cases, but the water channels are defined as lines and incorporate the analytic solution based on energy balance for a laminar flow in a tube (poiseuille flow, parabolic profile). The computation time is much shorter than the fluid simulation with Navier Stokes equations.

8. SIMULATION RESULTS AND DISCUSSION

The figure 5 shows the power density distribution inside the lignite and ceramic tube. There are 3 maximum located in the ceramic and lignite material (one in front of the aperture of the wave guide at the interface ceramic/lignite, one in the center, and one at the interface ceramic/lignite on the opposite side of the wave guide aperture). A maximum power density of about $100 \text{ MW}/\text{m}^3$ was achieved inside the lignite material.

The temperature field inside the lignite material and ceramic is shown in Fig. 6 after one hour of continuous running with briquettes moving from bottom to top with an average velocity of 2.5 cm/s which correspond to 75 briquettes per minute. The initial lignite temperature material was set to 80°C which is the temperature of the briquettes leaving the briquette press machine and entering in the inner tube of the applicator. The temperature field follows the power density distribution and is not uniform. The maximum temperature is close to 300°C . In this model, the vaporisation of water was not taken into account, and consequently the temperature is overestimated in this current model. The implication is not problematic for the design phase of this applicator because the thermal stress in the ceramic and aluminum parts of the applicator will be also overestimated. Using the heat source from the electromagnetic model, the

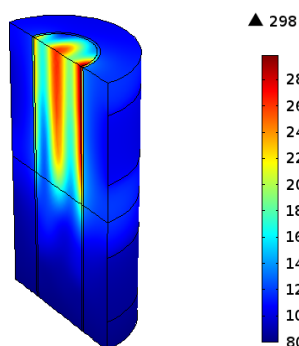


Fig. 6 Temperature [°C] distribution after 1 h of continuous running with a constant briquette translation velocity of $v = 2.5$ cm/s, corresponding to 75 briquettes per minute

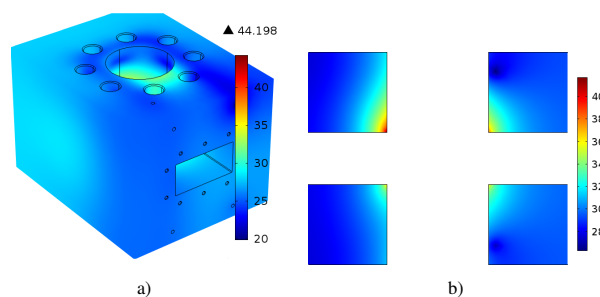


Fig. 7 Temperature after 1 h of continuous running with a water flow rate of 6 l/min in the aluminium block a) and in the middle plane of the block b)

temperature field inside the ceramic and metal block was computed for 6 l/min water flow rate. The figure 7 shows the temperature distribution inside the aluminum block (a) after 1 h of continuous running at 10 kW input power and in the middle plane of the aluminium block b). The white domain in the Fig. 7 is the wave guide filled with air. The ceramic and lignite material have also been hidden to see the temperature in this plane. For a flow rate of 6 l/min, the maximum temperature inside the steel block is about 44 °C in the aluminum block. For the same flow rate and input power, the maximal temperature calculated for a steel block is about 120 °C. The non uniformity of the temperature distribution (or temperature gradients) is much higher for the steel block than the aluminum block because of its lower thermal conductivity. This shows that thermal expansion can be mitigated by using an aluminum alloy together with a sufficient water flow. For this application, the use of Stainless steel is not recommended because of lower electrical and thermal conductivity than aluminum.

The maximum total Von Mises stress calculated with the thermo mechanical model (temperature field as an input) was about 40 – 60 MPa in the middle of the ceramic as shown in Fig. 8 a) (green and yellow range on the figure, the maximum is not physical since it corresponds to a corner singularity with fixed displacements). This stress value is well below the maximum tensile and compressive strength of the silicon nitride tube (more than 400 MPa for the tensile strength and 3000 MPa for the compressive strength). For certification reasons, the ceramic cylinder was also tested with high pressure water at 5 times the nominal pressure, i.e. 325 bars.

A modified model with the full geometry was used to compute the stress and displacement distribution inside the aluminum block. This block experiences stress from the inhomogeneous temperature distribution and from the 2 × 8 M22 screws used to connect the applicator to the flange for

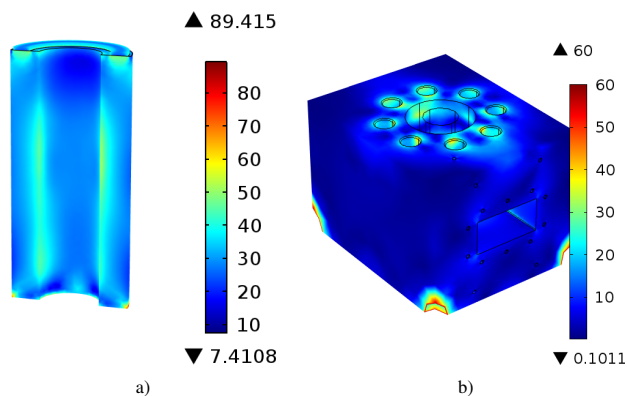


Fig. 8 Von Mises stress [MPa] in the ceramic Silicon nitride tube and inside the Aluminum block after 1 h of continuous running. Thermal stress, internal pressure, pressure from the gasket and forces from the screws are included in this model, high stress at the 4 corners are due to the fixed displacement boundary condition. The scale is limited to 60 MPa

a good sealing. After 1 h of continuous running, the maximal value for the Von Mises stress in steady state conditions was about 30 – 50 MPa in the vicinity of the screw thread insert (Fig. 8 b)). This value was well below the maximum tensile strength of Alumec 100 which is about 500 MPa. The maximum displacement was below 0.15 mm for a force of 60 kN per screw and flow rate of 6 l/min.

Overall, these thermo mechanical simulations have shown a good design of the applicator with stress level well below the maximal strength of the materials. In addition, the cooling circuit is essential in order to limit the maximal temperature and consequently the thermal expansion of the block.

9. EXPERIMENTAL RESULTS

The initial tests were performed without the briquetting press machine and the ceramic cylinder was simply filled with lignite briquettes. For these static conditions (no moving briquettes through the ceramic canal) few tests at a maximum power of 4 kW and for a maximum time duration of 10 s were performed. The temperature field just after microwave treatment was measured with a thermo camera as shown in Fig. 9. Surface temperature of about 100 °C were measured.

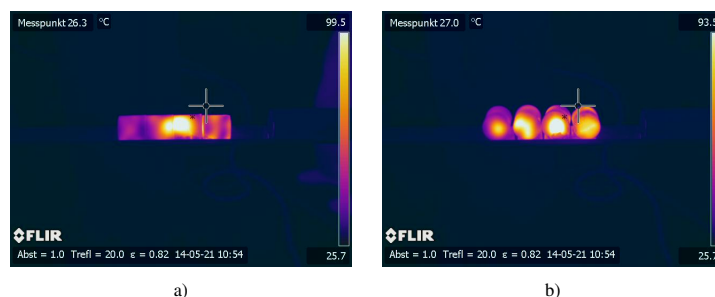


Fig. 9 Surface temperature obtained with a thermo camera, lateral and front view of 4 lignite briquette after microwave treatment, max temperature 99 °C

Additional tests were performed at atmospheric pressure with the applicator connected to the briquetting press and a maximal power of 10 kW could be used. The input power ranges from 0.5 – 10 kW with 0.5 kW step. The controlled software (Muegge MV220V) allows the control of the input power and the monitoring of the reflected power. Lignite briquettes were moving at various speeds between 50 to 75 briquettes

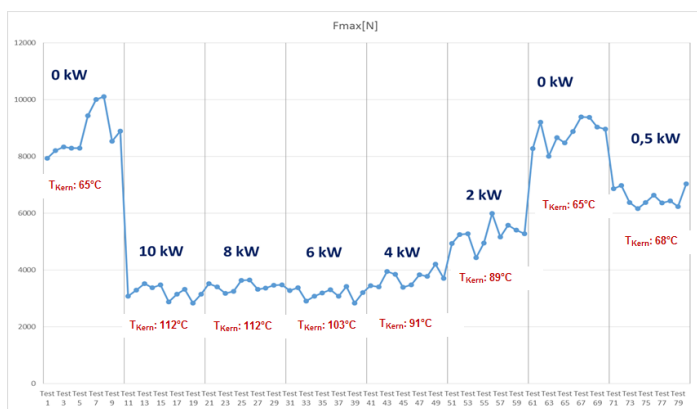


Fig. 10 Mean force [N] required to break the briquettes after microwave irradiation, for power ranging from 0 to 10 kW

per minute. Cracks formation with surface and core temperature of the lignite briquettes higher than 120 °C were measured.

A radial crack from the center to the outside was observed on all the microwave heated briquettes. Briquettes were heated at different power and were collected at the exit of the metallic tube (connected to the applicator) to measure the core temperature with a thermo coupled, after drilling a hole in the center. After that, they were put in a compressive stress machine, to measure the force required to induce breakage. The temperature was obtained from averaging 3 temperature measurements with 3 briquettes with the same input power and speed operating conditions. The figure 10 shows the force required to break the briquettes for different input power level together with the measured core temperature of the briquette (in red). It is interesting to see that even with a power of 500 W the briquettes are significantly weakened (9 kN for a briquette without microwave heating and 6 kN for a briquette heated with 500 W). The core temperature are all above 100 °C for power ranging from 6 to 10 kW. The temperature values should be taken cautiously because many sources of uncertainty exist (time during manipulation, hole drilling, resident time of the briquette in the metallic tube). Overall the Fig. 10 shows that microwave heating significantly increase the friability of the lignite briquettes. It is believed that a combination of thermal stress and pore pressure from water vaporization is the cause of thermal cracking.

10. CONCLUSION

A compact 10 kW microwave applicator for heating and thermal cracking of lignite briquettes was successfully designed and tested. With 10 kW input power, this applicator allows the heating of wet lignite briquettes (water content in mass of about ~ 15%) with temperature above 100 – 120 °C and with average briquettes velocities in the range 1.6 to 2.5 cm/s. The utilization of a silicon nitride tube is the key of this high pressure applicator because this material combines both a high mechanical strength and very low dielectric losses. In operation, the aluminum block incorporating an efficient water cooling circuit remains below 45 °C as predicted by the thermal simulations.

The preliminary strength measurements have shown a significant mechanical weakening of the briquettes under microwave heating. Internal cracks are created during fast microwave heating, it is not clear yet what is the dominant phenomenon between pore pressure from water expansion/vaporization and thermal stress due to temperature gradients. Additional experimental tests and measurements are planned to study fur-

ther the lignite coal material behaviour under fast microwave heating.

During the development phase of the applicator, the use of a sequentially coupled model between the electromagnetic, thermo fluid and mechanical physics allows the design of a reliable applicator with the desired specifications. It gives some good indications about the physical behaviour of the applicator in operation.

Finally, this applicator could be used for other lossy materials in liquid, solid, powder or granular form for continuous volumetric heating with internal pressure ranging from atmospheric pressure to 65 bars. Applications in chemistry and recycling are foreseen.

ACKNOWLEDGEMENTS

The authors would like to thank Dr. Heiner Gutte, TU-Bergakademie Freiberg, for the founding within the DER-project FE-35025755 "Studie zur berührungslosen Erwärmung und Schwächung von Kohlebriketts mit Mikrowellen für die Feststoffvergasung".

NOMENCLATURE

ρ	density (kg/m ³)
C_p	specific heat (J/kg · K)
k	thermal conductivity(W/(m.K))
σ	stress tensor (Pa)
ϵ	strain tensor (Pa)
I	identity tensor (Pa)
E	Young modulus (Pa)
ν	poisson ratio (-)
α	linear expansion coefficient (1/K)
ϵ_{rc}	relative complex permittivity (-)
μ_r	relative permeability (-)
\mathbf{E}	Electric field vector (V/m)
ω	pulsation (rad/s)
q	power density (W/m ³)
T	Temperature (K)
\mathbf{v}	average velocity of the briquette (m/s)
\mathbf{n}	normal vector to a given surface (-)
\mathbf{H}	magnetic field(H/m)
ϵ_0	permittivity of free space (F/m)
μ_0	permeability of free space(H/m)
∇	gradient operator
$\nabla \cdot$	divergent operator
$\nabla \times$	curl operator

REFERENCES

- Batar, T., 2004, "Theory and Applications of Microwave Energy in Communiton," *Euro Ceramics VIII*, 1399–1402.
<http://dx.doi.org/10.4028/www.scientific.net/KEM.264-268.1399>.
- Binner, E., Lester, E., Kingman, S., Dodds, C., Wu, J.R.T., Wardle, P., and Mathews, J., 2014, "A Review of Microwave Coal Processing," *Journal of Microwave Power and Electromagnetic Energy*, **48**, 35–60.
- Pickles, C., Gao, F., and S.Kelebek, 2014, "Microwave Drying of a Low Rank Sub Bitumous Coal," *Minerals Engineering*, **62**, 31–42.
<http://dx.doi.org/10.1016/j.mineng.2013.10.011>.
- Rosin, A., Schroder, H., and Repke, J., 2014, "Briquetting Press as Lock Free Continuous Feeding System for Pressurized gasifiers," *Fuel*, **116**, 871–878.
<http://dx.doi.org/10.1016/j.fuel.2013.03.024>.